Neurobiology of Disease

Cytochrome *c* Association with the Inner Mitochondrial Membrane Is Impaired in the CNS of G93A-SOD1 Mice

Ilias G. Kirkinezos,[1] **Sandra R. Bacman,**[2] **Dayami Hernandez,**[2] **Jose Oca-Cossio,**[2] **Laura J. Arias,**[3]
Miguel A. Perez-Pinzon,[2,3] **Walter G. Bradley,**[2,3] **and Carlos T. Moraes**[1,2,3]

Departments of [1]Cell Biology and Anatomy and [2]Neurology, and [3]Neuroscience Program, University of Miami School of Medicine, Miami, Florida 33136

A "gain-of-function" toxic property of mutant Cu–Zn superoxide dismutase 1 (SOD1) is involved in the pathogenesis of some familial cases of amyotrophic lateral sclerosis (ALS). Expression of a mutant form of the human SOD1 gene in mice causes a degeneration of motor neurons, leading to progressive muscle weakness and hindlimb paralysis. Transgenic mice overexpressing a mutant human SOD1 gene (G93A-SOD1) were used to examine the mitochondrial involvement in familial ALS. We observed a decrease in mitochondrial respiration in brain and spinal cord of the G93A-SOD1 mice. This decrease was significant only at the last step of the respiratory chain (complex IV), and it was not observed in transgenic wild-type SOD1 and nontransgenic mice. Interestingly, this decrease was evident even at a very early age in mice, long before any clinical symptoms arose. The effect seemed to be CNS specific, because no decrease was observed in liver mitochondria. Differences in complex IV respiration between brain mitochondria of G93A-SOD1 and control mice were abolished when reduced cytochrome *c* was used as an electron donor, pinpointing the defect to cytochrome *c*. Submitochondrial studies showed that cytochrome *c* in the brain of G93A-SOD1 mice had a reduced association with the inner mitochondrial membrane (IMM). Brain mitochondrial lipids, including cardiolipin, had increased peroxidation in G93A-SOD1 mice. These results suggest a mechanism by which mutant SOD1 can disrupt the association of cytochrome *c* with the IMM, thereby priming an apoptotic program.

Key words: amyotrophic lateral sclerosis; superoxide dismutase; mitochondria; cytochrome *c*; G93A-SOD1; lipid peroxidation

Introduction

Amyotrophic lateral sclerosis (ALS) is a fatal neurodegenerative disease that mainly affects motor neurons in cortex, brainstem, and spinal cord. Although the cause of ALS remains elusive, the presence of similar pathology in most ALS cases suggests that common pathogenetic mechanisms may lead to the development of the disease (Brown and Robberecht, 2001).

The majority of ALS cases are sporadic [sporadic ALS (SALS)]. However, in 5–10% of ALS cases, the disease is inherited as an autosomal dominant trait [familial ALS (FALS)]. Additionally, 15–20% of FALS cases are associated with point mutations of the superoxide dismutase 1 (SOD1) gene, which codes for one of the three isoforms of superoxide dismutase, the main scavenger enzyme of the superoxide radical (O_2·). There is evidence that oxidative damage may play a role in the pathogenesis of neuronal degeneration in both SALS and FALS (Ferrante et al., 1997; Bogdanov et al., 2000). Supportive evidence also came from studies showing that oxidative damage to proteins is increased in SALS patients (Bowling et al., 1993), FALS patients (Said Ahmed et al., 2000), and transgenic G93A-SOD1 mice (Liu et al., 1999; Warita

et al., 2001). Oxidative stress causes abnormal accumulation of FALS-related mutant SOD1 in transgenic *Caenhorabditis elegans* (Oeda et al., 2001). In the presence of oxidative stress, the rapid degradation of mutant SOD1 was inhibited, causing aggregates, which could mediate toxic effects (Bruijn et al., 1998). Copper atoms from SOD1 have been implicated in oxidative reactions (Carri et al., 2003). However, recent studies suggest that the copper at the active site of SOD1 is not involved in the pathogenesis (Subramaniam et al., 2002), although copper may still participate in peroxidative reactions (Bush, 2002).

Studies with transgenic mouse models of FALS indicate a dominant, gain-of-function effect of the FALS-associated SOD1 mutants (Gurney, 1994; Pardo et al., 1995; Wong et al., 1995). The nature of the function gained remains undetermined. The transgenic G93A-SOD1 mice express high levels of the mutated human SOD1 and develop a progressive motor neuron disease. There is growing evidence suggesting that mitochondria may be involved in the pathogenesis of ALS. In studies of spinal cord from SALS patients, a decrease in activity of cytochrome *c* oxidase (COX) was observed (Fujita et al., 1996; Borthwick et al., 1999). SOD1 mutant transgenic models showed prominent structural mitochondrial abnormalities (Wong et al., 1995; Kong and Xu, 1998). A significant fraction of SOD1 was localized to the mitochondrial intermembrane space, and mitochondrial respiration was found to be impaired in G93A-SOD1 CNS (Higgins et al., 2002; Mattiazzi et al., 2002). Finally, an apoptotic pathway involving mitochondrial changes has been associated with the G93A-SOD1, as well as with the SALS pathology (Guegan et al.,

2001). We investigated the role of mitochondrial function in this mouse model of ALS and found a link between mutant SOD1, respiratory impairment, and apoptosis.

Materials and Methods

Transgenic mice. G93A-SOD1 mice from the Gurney G1 line [B6SJL-TgN (SOD1-G93A)1 Gur] were obtained from The Jackson Laboratory (Bar Harbor, ME). G93A-SOD1 mice were bred in our animal facility in a FVB/N background, and the colony was maintained as an F5 (FVB/N) backcross. The development of symptoms and lifespan of the G93A-SOD1 of these transgenic animals were indistinguishable from the B6SJL background. Age of overt disease onset was ~90 d, and complete paralysis (death) was at 120 d for males and 130 d for females. Transgenic animals were identified for carrying the G93A-SOD1 allele by PCR of tail DNA, using primers for human SOD1 as recommended by The Jackson Laboratory. Nontransgenic littermates were used as age- and sex-matched controls. Additional controls consisted of mice overexpressing wild-type (WT) human SOD1 derived from the Gurney N29 line (Dal Canto and Gurney, 1995). The mice were housed at a virus antigen-free facility on a 12 hr light/dark cycle and were fed *ad libitum* with a standard diet. Unless used for tissue extractions, mice were killed when they could not right themselves up when placed on their back.

Mitochondrial isolation. We followed a modified procedure as described by Xiong et al. (1997). Animals were anesthetized with a mixture (in mg/ml: 42.8 ketamine, 8.6 xylanzine, and 1.4 acepromazine) at a dose of 10 ml/kg and decapitated, and their forebrains were placed into an ice-cold isolation buffer consisting of 250 mM sucrose, 10 mM HEPES, pH 7.4, 1 mg/ml bovine serum albumin, 0.5 mM EDTA, and 0.5 mM EGTA (SEE buffer). It has been reported that decapitation without anesthesia can affect mitochondrial function, possibly because of a catecholamine discharge (Dutkiewicz and Chelstowski, 1981). We found in pilot experiments that the anesthetic used at the doses indicated did not affect mitochondrial respiration. The minced tissue was placed in a handheld Teflon–glass homogenizer and was homogenized on ice for ~2 min (~5–10 strokes). After homogenization, it was diluted to 8 ml of SEE buffer. Subsequently, the homogenate was centrifuged at 2000 × *g* for 3 min in a refrigerated Sorvall RC2-B centrifuge (SS-34 rotor; Kendro Laboratory Products, Asheville, NC). The supernatant was carefully decanted and centrifuged at 12,000 × *g* for 8 min. The supernatant was discarded, and the pellet was resuspended in 10 ml of SEE buffer and centrifuged at 12,000 × *g* for 10 min. Finally, the pellet was resuspended in 10 ml of 250 mM sucrose and centrifuged at 12,000 × *g* for 10 min. This final pellet was carefully resuspended in 0.5 ml of 250 mM sucrose and used for subsequent experiments.

Mitochondrial function studies. Polarographic studies were performed as described previously (Barrientos et al., 1998) in 0.6 ml of standard medium (0.3 M mannitol, 10 mM KCl, 5 mM MgCl$_2$, 1 mg/ml BSA, and 10 mM KH$_2$PO$_4$, pH 7.4) with a Clark oxygen electrode in a micro-water-jacketed cell, magnetically stirred at 37°C (Hansatech Instruments, Norfolk, UK). The oxidation of pyruvate (6 mM) plus malate (3 mM) (site I substrates) was measured. The reaction was inhibited with rotenone (3 μM). The oxidation of succinate (5 mM) and glycerol-3-phosphate (4 mM) (site II substrates) was subsequently performed. After inhibition of complex III with antimycin A (AA) (1 μM), the oxidation of ascorbate (asc) (0.5 mM) plus *N,N,N′,N′*-tetramethyl-*p*-phenylenediamine (TMPD) (0.2 mM) through complex IV was measured. Approximately 150 μg of mitochondrial protein was used for each experiment. State 3 respiration (i.e., in the presence of ADP) was assessed for each substrate.

The measurement of the specific activity of the individual complexes of the electron transport chain (ETC) was performed spectrophotometrically essentially as described previously (Barrientos et al., 1998). The protein content in mitochondria samples was determined according to Bradford's method (Bradford, 1976).

Lactate measurement. Blood plasma from G93A-SOD1 transgenic mice, WT transgenic mice, and control mice was used to measure lactate levels in a glucose–lactate analyzer, YSI 2300 STAT Plus (YSI Life Sciences, Yellow Springs, OH).

Nitric oxide synthase activity assay. The conversion of H^3-arginine

to H^3-citrulline was analyzed as a measure of nitric oxide synthase (NOS) enzymatic activity. We used the NOSdetect assay kit (Stratagene, La Jolla, CA).

Immunodetection of mitochondrial proteins. Approximately 20 μg of mitochondrial proteins were resolved by SDS-PAGE (15% gels) and transferred onto polyvinylidene difluoride membranes (PerkinElmer Life Sciences, Boston, MA). Blots were blocked with 5% milk and probed with specific antibodies. The antibodies used were purchased from Molecular Probes (Eugene, OR), with the exception of the anti-cytochrome *c*, which was purchased from BD Biosciences Pharmingen (San Diego, CA). After washes, the membrane was treated with a secondary anti-rabbit or anti-mouse antibody conjugated to horseradish peroxidase. Detection was performed using the Phototope horseradish peroxidase Western blot detection kit (New England Biolabs, Beverly, MA).

Electron microscopy of COX-stained spinal cord sections. Three 115- to 125-d-old G93A-SOD1 mice and three age- and sex-matched nontransgenic control mice were prepared with 2% glutaraldehyde for additional histochemical analysis. The animals were initially perfused with 4 ml/min saline for 4–5 min and further perfused with 2% glutaraldehyde at the same rate of delivery for 15–20 min. Spinal cord and brain were surgically removed and immediately prepared for the histochemical reaction. We cut transverse sections of the lumbar enlargement of the spinal cords of a thickness of ~1 mm. The sections were incubated in 2% glutaraldehyde and 5% sucrose in 0.05 M PBS, pH 7.4, for 15 min at 4°C. To determine COX activity, sections were incubated in a solution of 5 mg of 3,3′-diaminobenzidine tetrahydrochloride, 9 ml of 0.05 M sodium phosphate buffer, pH 7.4, 1 ml of catalase (20 μm/ml), 10 mg of cytochrome *c*, and 750 mg of sucrose overnight at 37°C. Samples were fixed with 2% glutaraldehyde and 100 mM sucrose in a 0.05 M phosphate buffer for 24 hr and then were fixed with 1% OsO$_4$ in 0.1 M phosphate overnight at 4°C. Samples were then dehydrated in a series of ethanolic alcohols and infiltrated with a 1% mixture of propylene oxide and Epon-Araldite resin overnight at room temperature. Finally, samples were embedded in Epon-Araldite resin using a 64°C oven. Thin sections were obtained and were examined under a Philips (Hillsboro, OR) CM-10 electron microscope operating at 60 or 80 kV without poststaining.

Lipid peroxidation. Measurement of malondialdehyde (MDA), a marker of lipid peroxidation, was performed with the Bioxytech LPO-586 kit (OxisResearch, Portland, OR). Samples of homogenate and mitochondria from brains of G93A-SOD1 transgenic mice, WT SOD1 transgenic mice, and control mice were prepared as described previously. The last pellet was washed in 6 ml of PBS and centrifuged at 12,000 × *g* for 10 min. This final pellet was carefully resuspended in 0.3 ml of PBS. The protein content in homogenates and mitochondria samples was determined according to Bradford's method (Bradford, 1976). 10-*N*-nonyl acridine orange (NAO) (Molecular Probes), which binds with high affinity to cardiolipin, was used according to Petit et al. (1992) to estimate relative levels of cardiolipin peroxidation. Brain mitochondria from G93A-SOD1 transgenic mice and control mice were prepared as described previously, and the last pellet was washed in 6 ml of buffer A (in mM: 220 mannitol, 70 sucrose, 0.1 EDTA, and 10 HEPES, pH 7.4) and centrifuged at 12,000 × *g* for 10 min. This final pellet was resuspended in 0.3 ml of buffer A. The concentration of NAO used was 100 μM, and protein content was fixed at 200 μg/ml. Free dye was determined by absorbance at 495 nm.

Computer and statistical analysis. Experimental data were analyzed using the Excel statistical package (Microsoft, Redmond, WA). Student's *t* test (unpaired within each age group) was used for the comparison of two groups.

Results

Complex IV-driven respiration is decreased in brain mitochondria of G93A-SOD1 transgenic mice

To assess whether the electron transport function was altered in brain mitochondria from G93A-SOD1 mice, we studied the respiration rates of different complexes from the ETC. We isolated forebrain mitochondria from G93A-SOD1 mice and nontransgenic littermates as age- and sex-matched controls. After verify-
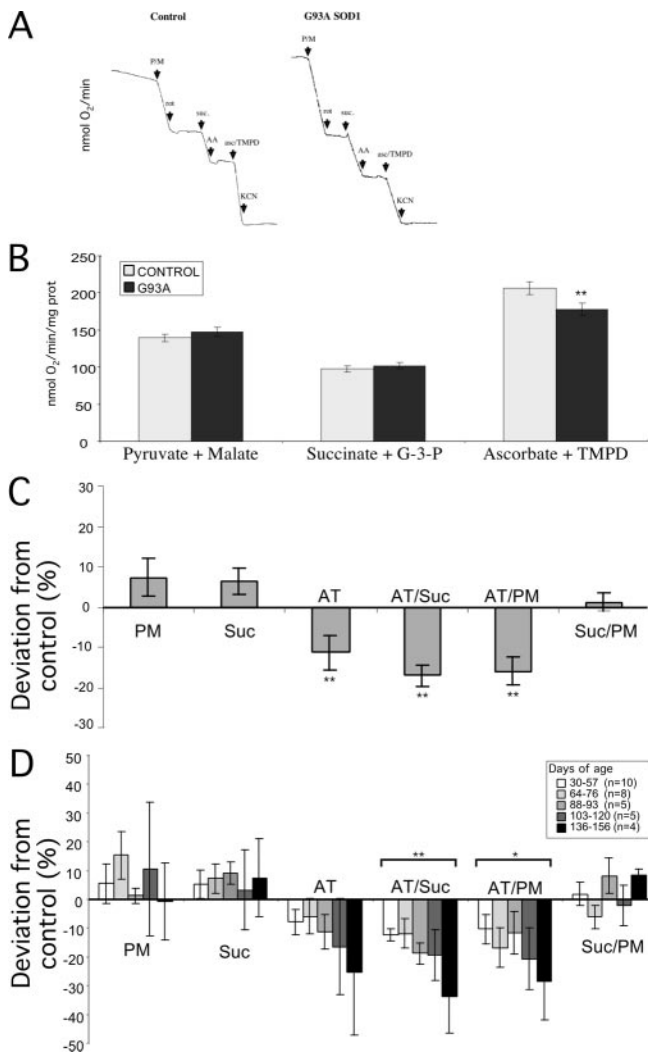
Figure 1. Oxygen consumption of brain mitochondria from G93A-SOD1 transgenic mice. *A,* Typical curves of oxygen consumption experiments measured by polarography. Mitochondrial respiration was stimulated by the following substrates: pyruvate–malate (P/M, PM), succinate (Suc), and asc–TMPD (AT). Inhibitors used were as follows: rotenone (rot), AA, and potassium cyanide (KCN). *B,* Bars express oxygen consumption observed in isolated brain mitochondria from control and G93A-SOD1 mice. *C,* The percentage of difference of brain mitochondria respiration rates of AT/Suc or AT/PM of G93A-SOD1 compared with controls. *B,C,* Results of 32 mice for each group (i.e., transgenic and littermate nontransgenic). *D,* Brain mitochondria respiration by age group. Brain mitochondria from the age groups described in the inset were studied as described above. Error bars indicate SEM. *$p < 0.01$; **$p < 0.001$. G-3-P, Glycerol-3-phosphate; prot, protein.

ing that the isolated mitochondria were coupled [i.e., fourfold to sevenfold (brain) and twofold to fivefold (spinal cord) increase in respiratory rates in the presence of ADP], we proceeded in measuring respiration with various substrates, which feed electrons to the ETC at different complexes (Trounce et al., 1996). Typical curves of state 3 respiration of brain mitochondria are shown (Fig. 1*A*). The three slopes correspond to respiration driven by electrons entering at different complexes (pyruvate–malate at complex I, succinate–glycerol-3-phosphate at complex II, and ascorbate–TMPD at complex IV, respectively).

In all of the age groups studied (spanning from 30 to 156 d of age), ascorbate–TMPD-driven respiration was significantly reduced ($p < 0.01$) in the samples from the affected mice compared with unaffected age-matched control mice, whereas the respiration rates driven by pyruvate–malate or succinate–

glycerol-3-phosphate did not differ significantly (Fig. 1*B,C*). Alternatively, we compared the ratios of TMPD–ascorbate (complex IV)-driven respiration over succinate–glycerol-3-phosphate (complex II)-driven respiration or over pyruvate–malate (complex I)-driven respiration. The complex IV/II and IV/I respiration ratios are accurate indicators of specific defects because of the internal control of the respiration and the elimination of the potential errors in protein measurements. Additionally, the complex IV/II ratio was a more reliable value than the complex IV/I ratio, because complex I is more sensitive to the mitochondrial isolation procedure than complexes II or IV are (Trounce et al., 1996). A consistent and significant decrease of complex IV-driven respiration in transgenic G93A-SOD1 mice brain mitochondria was revealed by the comparison of the complex IV/II and IV/I ratios. The mean decrease of complex IV respiration was 17% ($p < 0.0001$) and 16% ($p < 0.001$), respectively (Fig. 1*C*). No significant difference was observed for the II/I ratios.

**The asc–TMPD-driven respiration defect is observed in G93A-SOD1 mice from an early age**
Because ALS is a progressive disease with distinct stages, we separated the data in five age groups. The first two groups (30–57 and 64–76 d of age) represent the premuscle weakness stage of the disease (Kong and Xu, 1998), in which the muscle atrophy is not yet manifested. In this stage, however, subcellular events are initiated (e.g., vacuolization of mitochondria) to which mitochondrial function might be relevant. The third group (88–93 d of age) represents the start of the clinical signs of muscle weakness and the beginning of the rapid-decline phase of the disease. The fourth group (103–120 d of age) represents the slow-decline stage, in which muscle atrophy and weight loss are pronounced. Finally, the fifth group (136–156 d of age) represents the end stage of the disease, in which severe paralysis is observed. The analysis of the data showed that, in each and every group, there was a statistically significant decrease of ascorbate–TMPD-driven respiration from age-matched controls, which ranged from 12 to 34% (Fig. 1*D*). Although there was a trend for worsening with age, differences between the age groups were not statistically significant.

The asc–TMPD-driven decrease in respiration in G93A-SOD1 mice is specific for CNS tissue
The above results demonstrated a correlation between decreased asc–TMPD-driven respiration with the transgene G93A-SOD1 in mouse brain. To examine whether the mutant protein causes a similar decrease in mitochondria of other tissue, we isolated spinal cord ($n = 7$) and liver ($n = 24$) mitochondria from G93A-SOD1 and control mice and performed polarographic measurements as described previously. We observed a statistically significant decrease in the respiration of spinal cord mitochondria (35%; $p < 0.01$), which was very similar to the one observed for the brain mitochondria. In contrast, liver mitochondria did not show differences in any of the six respiration parameters analyzed (Fig. 2*A*). This finding suggests that the complex IV-driven respiration deficiency is specific to CNS tissue.

The ascorbate–TMPD-driven respiration deficiency is specific for the mutant SOD1
The mutant G93A-SOD1 retains its normal dismutase activity (Gurney, 1994). To examine whether the observed decrease of asc–TMPD-driven respiration is attributable to the increased levels of normal dismutase activity, we performed polarographic measurements of brain mitochondria from mice that overexpress
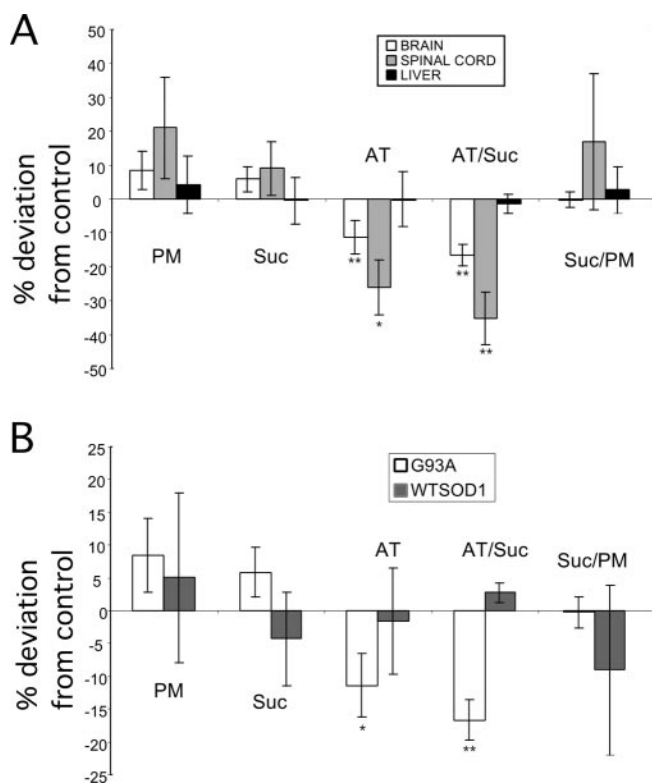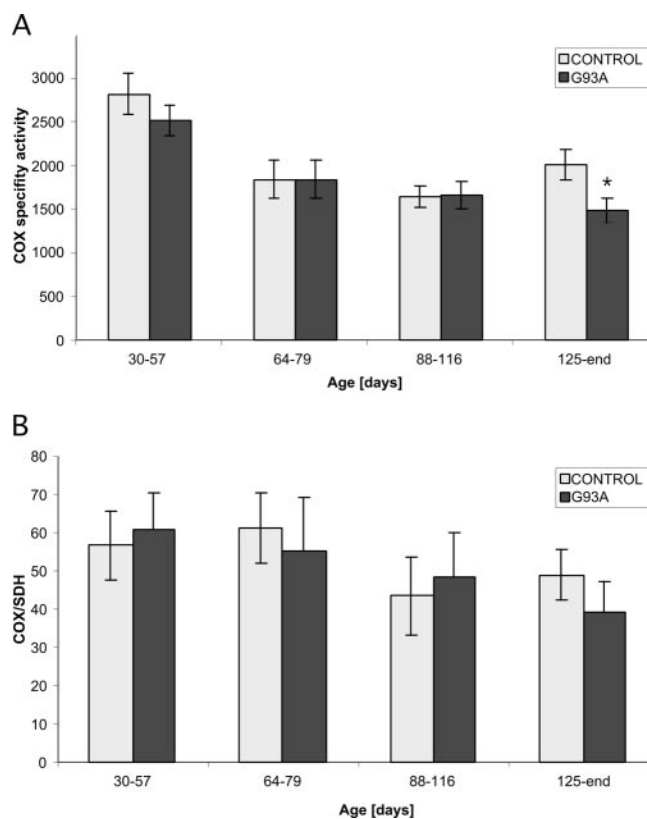
Figure 2. The complex IV-driven respiration defect is specific for CNS tissues of G93A-SOD1 mice. *A*, Comparison of differences between respiration of brain, spinal cord, and liver mitochondria. *B*, Comparison of differences between respiration of brain mitochondria from transgenic G93A-SOD1 and transgenic wild-type SOD1 mice. Data represented as in Figure 1. Spinal cord, $n = 7$ (70–120 d of age); liver, $n = 24$ (70–135 d of age); brain (same data as in Fig. 1; $n = 32$; 30–156 d of age). *$p < 0.05$; **$p < 0.01$. PM, Pyruvate–malate; Suc, succinate; AT, asc–TMPD.

Figure 3. Spectrophotometric measurements of mitochondrial enzyme activities in G93A-SOD1 spinal cord homogenates. *A*, The specific activity of cytochrome *c* oxidase in spinal cord mitochondria of G93A-SOD1 mice at different age groups. *B*, The ratios of cytochrome *c* oxidase over succinate dehydrogenase in the same samples. Although there was a small decrease in COX activity in the older mutant animals, there were no statistically significant changes in the COX/SDH ratios. Error bars indicate SEM. *$p < 0.05$ ($n = 30$).

the wild-type SOD1. Our data showed that overexpression of wild-type SOD1 did not affect the respiration parameters of the mitochondrial electron transport chain (Fig. 2*B*). Therefore, it seems that the gained toxic function of the mutant SOD1 is associated with the effect on mitochondrial respiration.

Analysis of mitochondrial enzyme activity in G93A-SOD1 mice

The asc–TMPD-driven respiration defect could be explained by a defect in cytochrome *c* oxidase. Using tissue homogenates, we performed spectrophotometric measurements of the activities of three mitochondrial enzymes: COX, succinate dehydrogenase (SDH), and citrate synthase. Animals were divided into four age groups (30–57, 64–79, 88–116, and 125–135 d of age) for both G93A-SOD1 transgenic and control mice. We observed a statistically significant decrease in cytochrome *c* oxidase activity in G93A-SOD1 spinal cord of ~25% ($p < 0.03$) (Fig. 3*A*). However, when the COX/SDH ratio was analyzed (Fig. 3*B*), there were no statistically significant differences between G93A-SOD1 and age-matched controls. In addition, no significant change was observed in the activity of citrate synthase in any age group when compared with age-matched controls (data not shown). Therefore, although there was a decrease in COX activity in G93A-SOD1 spinal cord, this defect was observed only at the end stage and is probably a consequence of mitochondrial degeneration. A similar pattern was observed for brain mitochondria, whereas liver mitochondria did not show a COX activity decrease, even in the older group (data not shown). We conclude that the small

and late reduction in COX activity in G93A-SOD1 CNS mitochondria does not explain the defect in asc–TMPD respiration observed in the different age groups.

We also did not observe significant changes in blood lactate of either young (50–60 d of age; 5.3 ± 0.5 mol/l; $n = 3$) or old (110–130 d of age; 6.1 ± 0.7 mol/l; $n = 6$) mice when compared with respective age-matched controls (young, 6.8 ± 1.2 mol/l; old, 6.1 ± 1.4 mol/l; data not shown).

Electron micrograph analysis of cytochrome *c* oxidase activity in spinal cord mitochondria

To further examine the activity of COX, we isolated spinal cord sections from the lumbar enlargement of G93A-SOD1 and non-transgenic age- and sex-matched control mice, and we stained histochemically for the activity of COX. As described previously (Kong and Xu, 1998), mitochondrial swelling, vacuolization, and loss of cristae were prominent in the G93A-SOD1 mice motor neuron cell bodies (Fig. 4). Mitochondria from motor neurons of the ventral horn of G93A-SOD1 mice did not exhibit a marked decrease in COX stain intensity relative to the corresponding mitochondria of control mice. We could observe that mitochondria from G93A-SOD1 mice had a "patchy" distribution of COX activity staining, with some areas of the membrane staining stronger than others. In contrast, the staining of mitochondrial membranes in controls was homogeneous (Fig. 4). The loss of cristae in affected animals could explain these observations, as

well as the mild decrease in COX-specific activity observed spectrophotometrically.

Levels of COX polypeptides do not correlate with decreased asc–TMPD in G93A-SOD1 brain

To test whether the observed decrease of asc–TMPD-driven respiration in brain was associated with decreased steady-state levels of the COX enzyme in the mitochondria, we prepared Western blots of mouse brain mitochondria samples. We used antibodies against the following polypeptides, which are part of the electron transport chain: COXI (a COX subunit encoded by the mitochondrial DNA), COXIV (a COX subunit encoded by the nuclear DNA), and SDH flavoprotein subunit. There were no significant changes in the steady-state levels of any of these polypeptides (Fig. 5), which suggests that the cause of the asc–TMPD

Figure 4. Electron micrographs of spinal cord sections stained for COX activity from G93A-SOD1 mice and controls. Spinal cord (lumbar enlargement) mitochondria from the G93A-SOD1 mice show features of structural defects (i.e., vacuolization and loss of cristae). The COX staining also showed a patchy pattern, suggesting intraorganelle heterogeneity in COX activity. Left, Control (CTRL) mouse. Right, G93A-SOD1 mouse. N, Nucleus.

defect in respiration was not a decrease in steady-state levels of COX components.
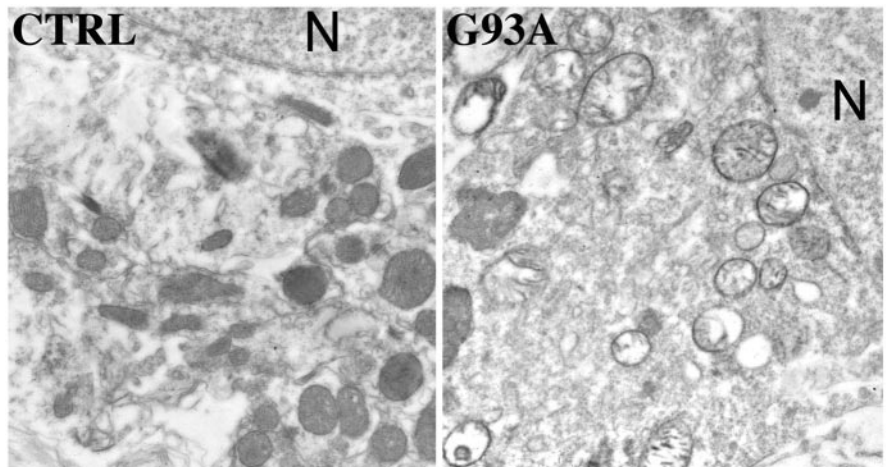
Together, the results suggest that the asc–TMPD respiration defect was not associated with a significant endogenous respiration defect or with COX defect in the CNS of G93A-SOD1 transgenic mice.

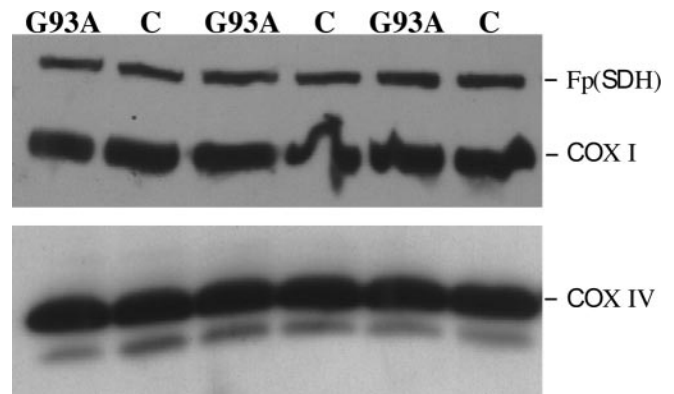## Total nitric oxide synthase activity is not changed in G93A-SOD1 mouse brain and spinal cord

A putative cause of a decreased complex IV-driven respiration could be the presence of elevated concentrations of NO. NO competes with oxygen by binding reversibly to the oxygen-binding site of the enzyme. An indirect method to measure levels of NO in a tissue is the measurement of NOS activity. We examined the levels of total NOS activity in mouse brain and spinal cord homogenates. This assay did not reveal any significant differences in the total NOS activity in either brain or spinal cord of G93A-SOD1 transgenic animals (data not shown).

Exogenous reduced cytochrome *c* restores complex IV respiration to normal levels

Ascorbate–TMPD donates electrons to cytochrome *c*, which in turn donates them to copper A, a prosthetic group of COX. To verify whether the partial defect in asc–TMPD respiration was caused by deficit–defect in cytochrome *c*, we measured electron transfer in mitoplasts. To prepare mitoplasts, the outer mitochondrial membrane (OMM) was disrupted by a mild hypotonic exposure as described previously (Barrientos et al., 2003), and the resulting mitoplasts were used in respiration experiments. Mitoplasts were still able to use succinate for respiration, which could be blocked by AA (Fig. 6A). Because of the "holes" in the outer membrane created by the hypotonic treatment, respiration could be stimulated by the addition of exogenous reduced cytochrome *c*, which donates electrons directly to complex IV (Fig. 6A). Subsequently, we compared the rates of oxygen consumption in mitoplasts from G93A-SOD1 spinal cord mitochondria with those from littermate controls. The previously observed asc–TMPD defect was not observed when reduced cytochrome *c* was used as a substrate for the mitochondrial respiration (Fig. 6), showing that the asc–TMPD defect was associated with a cytochrome *c*, and not cytochrome *c* oxidase, defect. Chemical modifications to


Figure 5. Western blot analysis of brain mitochondria. Antibodies directed against the mitochondrially encoded COXI, the nuclearly encoded COXIV, and the flavoprotein (Fp) of SDH were used to detect the respective polypeptides in brain mitochondrial homogenates. C, Nontransgenic littermate control.

cytochrome *c* have been reported to affect asc–TMPD respiration (Cassina et al., 2000). However, we were not able to detect nitrotyrosilation in immunoprecipitated cytochrome *c* using anti-nitrotyrosine antibodies (data not shown). Likewise, using Oxy-Blot (Chemicon, Temecula, CA), we were not able to detect increased oxidation of immunoprecipitated cytochrome *c* in G93A-SOD1 brain (data not shown).

Cytochrome *c* has decreased association with mitochondria in G93A-SOD1 transgenic mouse brain

In nonapoptotic cells, most cytochrome *c* remains associated with the inner mitochondrial membrane (IMM) after the disruption of the OMM (Barrientos et al., 2003). This is attributable to the association of cytochrome *c* with the respiratory complexes III and IV and with cardiolipin (Hoch, 1992). By lysing the OMM using a gentle hypotonic treatment, we observed that G93A-SOD1 brain mitochondria lost a disproportionately higher amount of cytochrome *c* than controls. This was documented by an internally controlled Western blot assay in which the levels of cytochrome *c* were normalized by the inner membrane flavoprotein of complex II (Fig. 7A). We determined that the brain
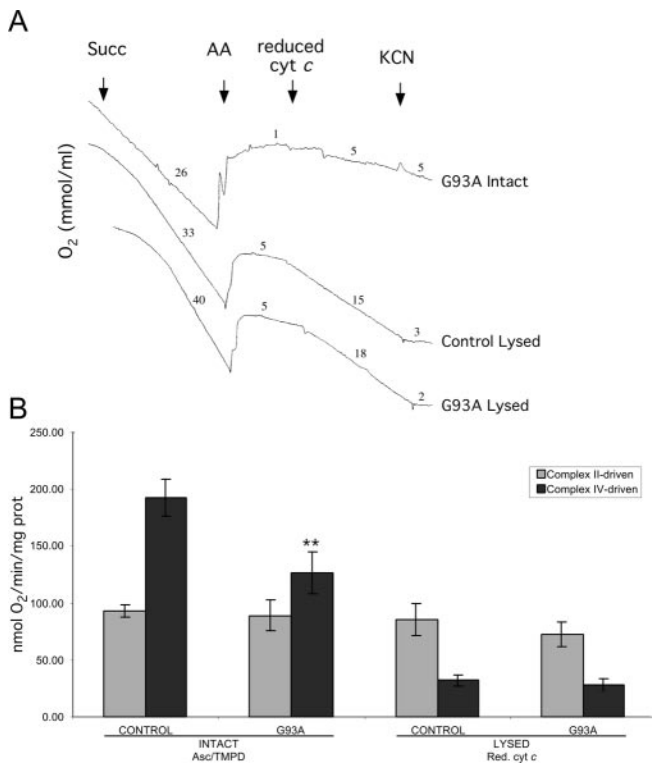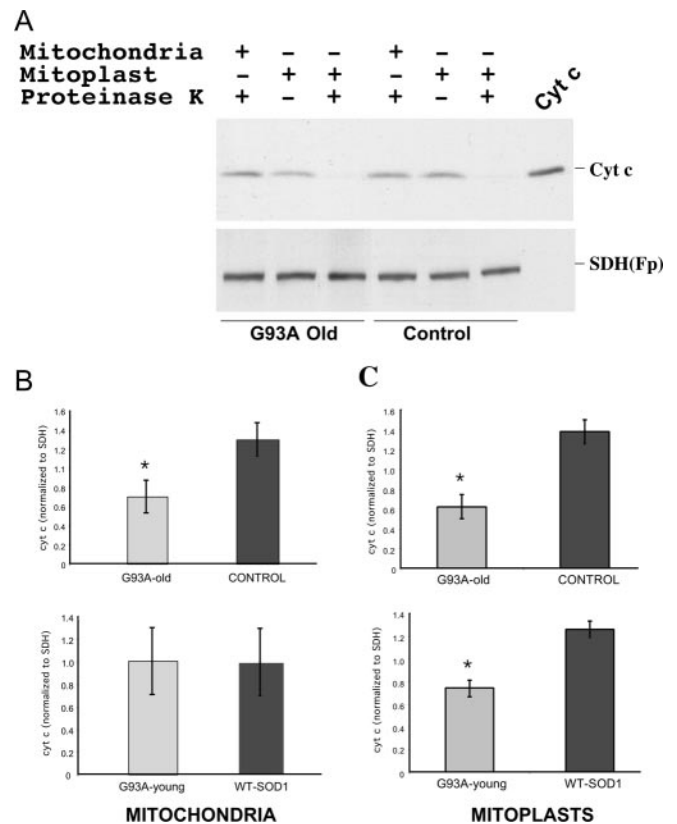
Figure 6. Complex IV-driven respiration is restored to control levels when reduced cytochrome c (Red. cyt c) is used as an electron donor. Outer membranes of spinal cord mitochondria were lysed by a mild hypotonic shock (as described in Materials and Methods), and oxygen consumption was measured as described previously. A, Traces of intact and lysed mitochondria respiration. Reduced cytochrome c can donate electrons directly to complex IV, but only if it has access to the intermembrane space. B, The defect in asc–TMPD respiration observed in G93A-SOD1 spinal cord mitochondria cannot be observed in lysed mitochondria when asc–TMPD is replaced with reduced cytochrome c. **$p < 0.01$. Succ, Succinate; KCN, potassium cyanide; prot, protein.

Figure 7. Cytochrome c (Cyt c) levels in isolated mitochondria and mitoplasts of G93A-SOD1 brain. A, A representative Western blot experiment of inner mitochondrial membrane-associated cytochrome c detection, measured as a ratio to SDH [flavoprotein (Fp)]. The disappearance of cytochrome c signal in the proteinase K-treated mitoplasts demonstrates that the outer mitochondrial membrane is ruptured. SDH is used as loading control. B, C, Measurements of cytochrome c presence in mitochondria (B) and mitoplasts (C) in symptomatic [old (110–130 d); n = 5], asymptomatic [young (50–60 d); n = 4] G93A-SOD1, nontransgenic control (n = 5), and wild-type SOD1 (n = 4) mouse brains. *$p < 0.01$.

mitochondria of old (110–130 d) G93A-SOD1 mice had reduced levels of cytochrome c (Fig. 7B, top). The difference from controls became higher when the OMM was disrupted (Fig. 7C, top). Brain mitochondria of young (50–60 d) G93A-SOD1 mice did not have reduced levels of cytochrome c in mitochondria (Fig. 7B, bottom). However, after the rupture of the outer membrane, a significantly larger amount of cytochrome c (~40%) was lost from the mitoplasts (Fig. 7C, bottom). Therefore, both presymptomatic and symptomatic G93A-SOD1 mice had decreased association of cytochrome c with the IMM.

It is possible that the mutant SOD1 "traps" cytochrome c. We immunoprecipitated cytochrome c from purified brain mitochondria and tested whether SOD1 was pulled down with the former. Although we observed a strong SOD1 band in Western blots of immunoprecipitates, in both the G93A-SOD1 and wild-type SOD1 models, preimmune serum also pulled down SOD1, making the result inconclusive (data not shown). Therefore, although we could not demonstrate such direct association, we cannot exclude the possibility that these two proteins interact.

Oxidation of the IMM lipids in G93A-SOD1 transgenic mouse brain is associated with cytochrome c dissociation
It has been shown that oxidation of the IMM lipids, particularly cardiolipin, leads to cytochrome c dissociation (Petrosillo et al., 2003). We tested whether the brain mitochondrial membranes were preferentially oxidized in G93A-SOD1 transgenic mice. The

levels of the lipid peroxidation metabolite MDA were significantly higher in mitochondria when compared with total brain homogenate of both asymptomatic and symptomatic G93A-SOD1 mice (Fig. 8). There were no significant differences between young and old G93A-SOD1 brains. Wild-type SOD1 transgenic brain did not have alterations in lipid peroxidation (Fig. 8A). Likewise, cardiolipin oxidation, measured by decreased binding of NAO, was significantly increased in G93A-SOD1 transgenic brain mitochondria of symptomatic G93A-SOD1 mice (Fig. 8B).

Discussion
We studied mitochondrial function in G93A-SOD1 mice to explore the potential role of mitochondria in the pathogenesis of ALS. When we analyzed the efficiency of electron transfer and the resulting oxygen consumption, complex IV-driven respiration was specifically affected in all of the age groups examined and long before the clinical onset of the disease. Spinal cord mitochondria were more affected than brain mitochondria, which would correlate with the disease process. We were unable to find a defect in asc–TMPD respiration in liver mitochondria of G93A-SOD1 mice or in the CNS of wild-type SOD1 transgenic mice. Because motor neurons make up only ~1% of neuronal cells in the CNS, if the partial dysfunction in asc–TMPD respiration was restricted to motor neurons, it is unlikely that it would be de-
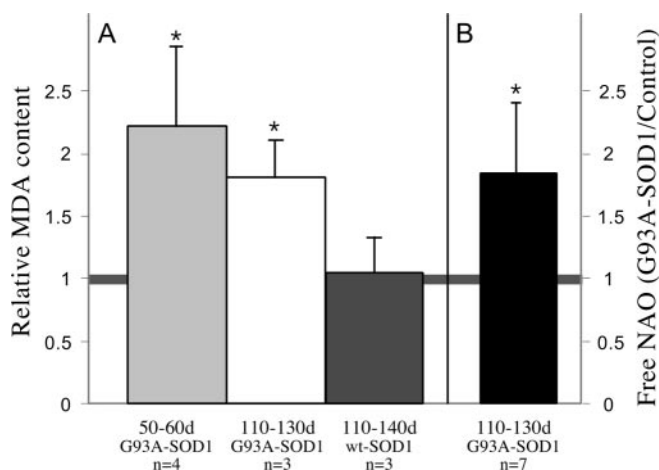
Figure 8. Lipid peroxidation in mitochondrial membranes is relatively increased in G93A-SOD1 brain. *A*, The measurement of MDA as a ratio of the levels in isolated mitochondria to that in total brain homogenates. The preferential oxidation of mitochondrial membranes in brain was observed for both young (50–60 d) and old (110–130 d) mice. The wild-type overexpressors (110–140 d of age) did not show the same increase. *B*, The levels of free NAO (a cardiolipin binding dye), expressed as a ratio of G93A over littermate controls. Unbound NAO levels were increased in G93A-SOD1 brain of 110- to 130-d-old mice, suggesting increased cardiolipin oxidation. Error bars indicate SD. *$p < 0.05$.

tected by our experimental approach. Therefore, our results suggest a generalized impairment in complex IV-driven respiration throughout the CNS.

We observed a defect in the activity of cytochrome *c* oxidase in the brain and spinal cord of G93A-SOD1 mice at the end stage. A defect in the activity of oxidative phosphorylation enzymes was also observed by others (Jung et al., 2002; Mattiazzi et al., 2002). This defect was associated with morphologically abnormal mitochondria and with a patchy distribution of COX activity in the IMM. Morphological abnormalities of mitochondria have been observed previously (Kong and Xu, 1998; Kato et al., 2004). The temporal expression of these enzyme defects suggests that they are late markers of the disease, which is probably a consequence of mitochondrial degeneration. The preferential decrease in COX activity may be associated with cardiolipin peroxidation (see below). Cardiolipin is necessary for COX activity (Hoch, 1992), and, in late-stage animals, its oxidized fraction may be high enough to disturb COX activity. Mattiazzi et al. (2002) detected defects in mitochondrial respiration in brain and spinal cord of 120-d-old G93A-SOD1 transgenic mice. Oxidative phosphorylation complex enzyme defects were also observed in spinal cord but not in brain. As mentioned above, we suggest that these defects are mostly caused by the neurodegenerative process, which is more pronounced in spinal cord.

By using reduced cytochrome *c* as an electron donor, we were able to bypass the complex IV respiration defect, narrowing the problem to cytochrome *c*. A series of recent reports showed that SOD1 in this transgenic model is present in the mitochondrial intermembrane space at concentrations that are equal to those found in the cytosol (Jaarsma et al., 2001; Higgins et al., 2002; Mattiazzi et al., 2002). Coincidentally, this is the same compartment in which cytochrome *c* is located. Targeting of mutant SOD1 to mitochondria exacerbates neuronal death, release of cytochrome *c* from mitochondria, and caspase activation (Takeuchi et al., 2002).

Chemical modifications would reduce cytochrome *c* function (Cassina et al., 2000), but we could not detect increased nitroty-

rosilation or increased carbamyl residues in G93A-SOD1 brain immunoprecipitated cytochrome *c*. Our results could also be explained by a decrease in cytochrome *c* levels. Guegan et al. (2001) showed in a series of experiments that cytochrome *c* levels were increased in the cytosol and slightly decreased in mitochondria of motor neurons from G93A-SOD1 mice. We were able to observe a significant cytochrome *c* loss from old (110–120 d) G93A-SOD1 brain mitochondria but not from mitochondria of younger mice. However, both old and young G93A-SOD1 brain mitochondria showed decreased cytochrome *c* association with the IMM. A series of publications have demonstrated that cytochrome *c* association with the IMM depends on the integrity of IMM lipids, particularly cardiolipin (Hoch, 1992; Shidoji et al., 1999; Nomura et al., 2000). We and others (Mattiazzi et al., 2002) showed increased lipid peroxidation in mitochondrial of G93A-SOD1 mice. We also showed that cardiolipin had a reduced capacity to bind NAO, reflecting peroxidation or loss of cardiolipin (Garcia Fernandez et al., 2004), either of which would compromise the binding of cytochrome *c* to cardiolipin (Paradies et al., 2000) and would be a prelude to apoptosis (Kirkland et al., 2002; Iverson and Orrenius, 2004; Nakagawa, 2004). Several studies demonstrated that cytochrome *c* release from mitochondria during apoptosis is a two-step process consisting of the dissociation of this protein from cardiolipin, followed by permeabilization of the outer membrane (McMillin and Dowhan, 2002; Petrosillo et al., 2003; Yuan et al., 2003). It is possible that, in our mouse model, we witnessed the first step (increased dissociation) in younger asymptomatic mice and the second step (release) in older symptomatic mice. Accordingly, caspase activation increases with age in the G93A-SOD1 mouse model (Guegan et al., 2001).

A number of additional recent observations are compatible with our findings. Higgins et al. (2003) have shown that the mutant SOD1 induces extension and leakage of the outer mitochondrial membrane and expansion of the intermembrane space. This mitochondrial "vacuolation by intermembrane space expansion" was suggested to potentiate apoptosis. Menzies et al. (2002) showed that NSC34 cells transfected with the G93A or G37R versions of SOD1 had a defect in complexes II and IV and were more sensitive to cell death. Because we observed a generalized increase in cytochrome *c*–IMM dissociation in the G93A-SOD1 brain, we propose that, although this elevated dissociation is present in different CNS cell types, it makes only motor neurons prone to apoptosis. A potential reason for this could be the higher influx of Ca^{2+} caused by glutamate signaling in motor neurons, which could alter mitochondrial structure. Abnormalities of the glutamate transporter EAAT2 (excitatory amino acid transporter 2) can increase postsynaptic glutamate concentrations (Lin et al., 1998; Heath and Shaw, 2002), providing such a stress. In addition, motor neurons lack important Ca^{2+} buffering proteins such as parvalbumin and calbindin D28K (Ince et al., 1993).

Two recent reports suggest that mutant SOD1 forms aggregates, located mostly at the cytoplasmic face of spinal cord outer mitochondrial membrane and possibly associated with mitochondrial import pores (Liu et al., 2004) or Bcl-2 (Pasinelli et al., 2004). The presence of SOD1 (wild-type or mutant) in brain mitochondria has been questioned in these reports. Although Liu et al. (2004) did not detect wild-type or G85R SOD1 in brain mitochondria, they did detect the G37R, G93A, and G127X forms of SOD1. The G85R is the lowest abundant SOD1 in the available animal models, and its presence in brain mitochondria may be more difficult to detect.

Based on what we currently know, there are at least two possible models for the cytochrome *c* dissociation: (1) G93A-SOD1

participates in the oxidation of cardiolipin, possibly mediated by copper atoms bound to the surface of the mutant SOD1 (i.e., not in the catalytic site) (Bush, 2002; Subramaniam et al., 2002), and (2) misfolded G93A-SOD1 aggregates with other mitochondrial components, affecting mitochondrial homeostasis and increasing cardiolipin peroxidation. In fact, Kato et al. (2004) showed that, in ALS patients and SOD1 transgenic rat models of ALS, SOD1 immunoreactive material colocalizes with thioredoxin peroxidase and glutathione peroxidase 1 in neuronal Lewy body-like hyaline inclusions (Kato et al., 2004), suggesting that SOD1 aggregates may affect the cellular reactive oxygen species (ROS) scavenging system. We favor a model in which aggregation of mutant SOD1 with mitochondrial components, possibly associated with ROS metabolism, leads to increased cardiolipin oxidation, increasing cytochrome *c* dissociation from the IMM. At this point, the cell may become more susceptible to apoptotic stresses that induce matrix swelling or affect the integrity of the outer mitochondrial membrane. A spike of Ca^{2+} influx in the cytosol could provide such stress. Also in support of this mechanism, cyclosporine A, an inhibitor of the mitochondrial permeability transition pore, does confer some protection to G93A-SOD1 mice and possibly humans (Appel et al., 1988; Keep et al., 2001; Kirkinezos et al., 2004). In addition, treatment of two ALS mouse models (including the G93A-SOD1 transgenic) with creatine increased the life expectancy of the animals (Klivenyi et al., 1999). Creatine administration seems to stabilize the mitochondrial creatine kinase and inhibit opening of the mitochondrial transition pore (Klivenyi et al., 1999).

Why is the expression of mutant SOD1 in glial cells required to cause an ALS phenotype (Clement et al., 2003)? A putative explanation for the requirement of mutant SOD1 in other cells is that an environmental metabolic stress is also necessary to trigger mitochondrial apoptosis in motor neurons. Excess of glutamate at the synapse leads to excitotoxic events, including increased intracellular Ca^{2+} influx, a well established trigger of mitochondrial swelling and permeability transition. At this point, it is unclear how broad the role of cytochrome *c* dissociation from the IMM in neurodegenerative processes is. Complex IV-driven respiration decrease has also been observed in wobbler mice, a naturally occurring model of motor neuron degeneration (Xu et al., 2001).

In conclusion, cytochrome *c* dissociation from the IMM may have an important role in the pathogenesis of motor neuron degenerations. Although the mechanisms involved are not clear, the fact that apoptosis, asc–TMPD respiration, and COX deficiency have been observed in several neurodegenerative processes suggests that cytochrome *c* dissociation may be a common apoptotic trigger in these conditions. Therefore, identifying the trigger of cytochrome *c*–IMM dissociation from the IMM could provide important clues to decipher molecular events before the onset of disease.

References

Appel SH, Stewart SS, Appel V, Harati Y, Mietlowski W, Weiss W, Belendiuk GW (1988) A double-blind study of the effectiveness of cyclosporine in amyotrophic lateral sclerosis. Arch Neurol 45:381–386.

Barrientos A, Kenyon L, Moraes CT (1998) Human xenomitochondrial cybrids. Cellular models of mitochondrial complex I deficiency. J Biol Chem 273:14210–14217.

Barrientos A, Pierre D, Lee J, Tzagoloff A (2003) Cytochrome oxidase assembly does not require catalytically active cytochrome C. J Biol Chem 278:8881–8887.

Bogdanov M, Brown RH, Matson W, Smart R, Hayden D, O'Donnell H, Flint Beal M, Cudkowicz M (2000) Increased oxidative damage to DNA in ALS patients. Free Radic Biol Med 29:652–658.

Borthwick GM, Johnson MA, Ince PG, Shaw PJ, Turnbull DM (1999) Mitochondrial enzyme activity in amyotrophic lateral sclerosis: implications for the role of mitochondria in neuronal cell death. Ann Neurol 46:787–790.

Bowling AC, Schulz JB, Brown Jr RH, Beal MF (1993) Superoxide dismutase activity, oxidative damage, and mitochondrial energy metabolism in familial and sporadic amyotrophic lateral sclerosis. J Neurochem 61:2322–2325.

Bradford MM (1976) A rapid and sensitive method for the quantitation of microgram quantities of protein utilizing the principle of protein-dye binding. Anal Biochem 72:248–254.

Brown Jr RH, Robberecht W (2001) Amyotrophic lateral sclerosis: pathogenesis. Semin Neurol 21:131–139.

Bruijn LI, Houseweart MK, Kato S, Anderson KL, Anderson SD, Ohama E, Reaume AG, Scott RW, Cleveland DW (1998) Aggregation and motor neuron toxicity of an ALS-linked SOD1 mutant independent from wild-type SOD1. Science 281:1851–1854.

Bush AI (2002) Is ALS caused by an altered oxidative activity of mutant superoxide dismutase? Nat Neurosci 5:919–920.

Carri MT, Ferri A, Cozzolino M, Calabrese L, Rotilio G (2003) Neurodegeneration in amyotrophic lateral sclerosis: the role of oxidative stress and altered homeostasis of metals. Brain Res Bull 61:365–374.

Cassina AM, Hodara R, Souza JM, Thomson L, Castro L, Ischiropoulos H, Freeman BA, Radi R (2000) Cytochrome c nitration by peroxynitrite. J Biol Chem 275:21409–21415.

Clement AM, Nguyen MD, Roberts EA, Garcia ML, Boillee S, Rule M, McMahon AP, Doucette W, Siwek D, Ferrante RJ, Brown Jr RH, Julien JP, Goldstein LS, Cleveland DW (2003) Wild-type nonneuronal cells extend survival of SOD1 mutant motor neurons in ALS mice. Science 302:113–117.

Dal Canto MC, Gurney ME (1995) Neuropathological changes in two lines of mice carrying a transgene for mutant human Cu, Zn SOD, and in mice overexpressing wild type human SOD: a model of familial amyotrophic lateral sclerosis (FALS). Brain Res 676:25–40.

Dutkiewicz T, Chelstowski K (1981) Comparative studies on the influence of decapitation, ketamine and thiopental anesthesia on rat heart mitochondria. Basic Res Cardiol 76:136–143.

Ferrante RJ, Browne SE, Shinobu LA, Bowling AC, Baik MJ, MacGarvey U, Kowall NW, Brown Jr RH, Beal MF (1997) Evidence of increased oxidative damage in both sporadic and familial amyotrophic lateral sclerosis. J Neurochem 69:2064–2074.

Fujita K, Yamauchi M, Shibayama K, Ando M, Honda M, Nagata Y (1996) Decreased cytochrome c oxidase activity but unchanged superoxide dismutase and glutathione peroxidase activities in the spinal cords of patients with amyotrophic lateral sclerosis. J Neurosci Res 45:276–281.

Garcia Fernandez MI, Ceccarelli D, Muscatello U (2004) Use of the fluorescent dye 10-N-nonyl acridine orange in quantitative and location assays of cardiolipin: a study on different experimental models. Anal Biochem 328:174–180.

Guegan C, Vila M, Rosoklija G, Hays AP, Przedborski S (2001) Recruitment of the mitochondrial-dependent apoptotic pathway in amyotrophic lateral sclerosis. J Neurosci 21:6569–6576.

Gurney ME (1994) Transgenic-mouse model of amyotrophic lateral sclerosis. N Engl J Med 331:1721–1722.

Heath PR, Shaw PJ (2002) Update on the glutamatergic neurotransmitter system and the role of excitotoxicity in amyotrophic lateral sclerosis. Muscle Nerve 26:438–458.

Higgins C, Jung C, Ding H, Xu Z (2002) Mutant Cu, Zn superoxide dismutase that causes motoneuron degeneration is present in mitochondria in the CNS. J Neurosci 22:RC215(1–6).

Higgins CM, Jung C, Xu Z (2003) ALS-associated mutant SOD1G93A causes mitochondrial vacuolation by expansion of the intermembrane space and by involvement of SOD1 aggregation and peroxisomes. BMC Neurosci 4:16.

Hoch FL (1992) Cardiolipins and biomembrane function. Biochim Biophys Acta 1113:71–133.

Ince P, Stout N, Shaw P, Slade J, Hunziker W, Heizmann CW, Baimbridge KG (1993) Parvalbumin and calbindin D-28k in the human motor system and in motor neuron disease. Neuropathol Appl Neurobiol 19:291–299.

Iverson SL, Orrenius S (2004) The cardiolipin-cytochrome *c* interaction and the mitochondrial regulation of apoptosis. Arch Biochem Biophys 423:37–46.

Jaarsma D, Rognoni F, van Duijn W, Verspaget HW, Haasdijk ED, Holstege JC (2001) CuZn superoxide dismutase (SOD1) accumulates in vacuolated mitochondria in transgenic mice expressing amyotrophic lateral sclerosis-linked SOD1 mutations. Acta Neuropathol (Berl) 102:293–305.

Jung C, Higgins CM, Xu Z (2002) Mitochondrial electron transport chain complex dysfunction in a transgenic mouse model for amyotrophic lateral sclerosis. J Neurochem 83:535–545.

Kato S, Saeki Y, Aoki M, Nagai M, Ishigaki A, Itoyama Y, Kato M, Asayama K, Awaya A, Hirano A, Ohama E (2004) Histological evidence of redox system breakdown caused by superoxide dismutase 1 (SOD1) aggregation is common to SOD1-mutated motor neurons in humans and animal models. Acta Neuropathol (Berl) 107:149–158.

Keep M, Elmer E, Fong KS, Csiszar K (2001) Intrathecal cyclosporin prolongs survival of late-stage ALS mice. Brain Res 894:327–331.

Kirkinezos IG, Hernandez D, Bradley WG, Moraes CT (2004) An ALS mouse model with a permeable blood-brain barrier benefits from systemic cyclosporine A treatment. J Neurochem 88:821–826.

Kirkland RA, Adibhatla RM, Hatcher JF, Franklin JL (2002) Loss of cardiolipin and mitochondria during programmed neuronal death: evidence of a role for lipid peroxidation and autophagy. Neuroscience 115:587–602.

Klivenyi P, Ferrante RJ, Matthews RT, Bogdanov MB, Klein AM, Andreassen OA, Mueller G, Wermer M, Kaddurah-Daouk R, Beal MF (1999) Neuroprotective effects of creatine in a transgenic animal model of amyotrophic lateral sclerosis. Nat Med 5:347–350.

Kong J, Xu Z (1998) Massive mitochondrial degeneration in motor neurons triggers the onset of amyotrophic lateral sclerosis in mice expressing a mutant SOD1. J Neurosci 18:3241–3250.

Lin CL, Bristol LA, Jin L, Dykes-Hoberg M, Crawford T, Clawson L, Rothstein JD (1998) Aberrant RNA processing in a neurodegenerative disease: the cause for absent EAAT2, a glutamate transporter, in amyotrophic lateral sclerosis. Neuron 20:589–602.

Liu D, Wen J, Liu J, Li L (1999) The roles of free radicals in amyotrophic lateral sclerosis: reactive oxygen species and elevated oxidation of protein, DNA, and membrane phospholipids. FASEB J 13:2318–2328.

Liu J, Lillo C, Jonsson PA, Velde CV, Ward CM, Miller TM, Subramaniam JR, Rothstein JD, Marklund S, Andersen PM, Brannstrom T, Gredal O, Wong PC, Williams DS, Cleveland DW (2004) Toxicity of familial ALS-linked SOD1 mutants from selective recruitment to spinal mitochondria. Neuron 43:5–17.

Mattiazzi M, D'Aurelio M, Gajewski CD, Martushova K, Kiaei M, Beal MF, Manfredi G (2002) Mutated human SOD1 causes dysfunction of oxidative phosphorylation in mitochondria of transgenic mice. J Biol Chem 277:29626–29633.

McMillin JB, Dowhan W (2002) Cardiolipin and apoptosis. Biochim Biophys Acta 1585:97–107.

Menzies FM, Cookson MR, Taylor RW, Turnbull DM, Chrzanowska-Lightowlers ZM, Dong L, Figlewicz DA, Shaw PJ (2002) Mitochondrial dysfunction in a cell culture model of familial amyotrophic lateral sclerosis. Brain 125:1522–1533.

Nakagawa Y (2004) Initiation of apoptotic signal by the peroxidation of cardiolipin of mitochondria. Ann NY Acad Sci 1011:177–184.

Nomura K, Imai H, Koumura T, Kobayashi T, Nakagawa Y (2000) Mitochondrial phospholipid hydroperoxide glutathione peroxidase inhibits the release of cytochrome c from mitochondria by suppressing the peroxidation of cardiolipin in hypoglycaemia-induced apoptosis. Biochem J 351:183–193.

Oeda T, Shimohama S, Kitagawa N, Kohno R, Imura T, Shibasaki H, Ishii N (2001) Oxidative stress causes abnormal accumulation of familial amyotrophic lateral sclerosis-related mutant SOD1 in transgenic *Caenorhabditis elegans*. Hum Mol Genet 10:2013–2023.

Paradies G, Petrosillo G, Pistolese M, Ruggiero FM (2000) The effect of reactive oxygen species generated from the mitochondrial electron transport chain on the cytochrome c oxidase activity and on the cardiolipin content in bovine heart submitochondrial particles. FEBS Lett 466:323–326.

Pardo CA, Xu Z, Borchelt DR, Price DL, Sisodia SS, Cleveland DW (1995) Superoxide dismutase is an abundant component in cell bodies, dendrites, and axons of motor neurons and in a subset of other neurons. Proc Natl Acad Sci USA 92:954–958.

Pasinelli P, Belford ME, Lennon N, Bacskai BJ, Hyman BT, Trotti D, Brown Jr RH (2004) Amyotrophic lateral sclerosis-associated SOD1 mutant proteins bind and aggregate with Bcl-2 in spinal cord mitochondria. Neuron 43:19–30.

Petit JM, Maftah A, Ratinaud MH, Julien R (1992) 10*N*-nonyl acridine orange interacts with cardiolipin and allows the quantification of this phospholipid in isolated mitochondria. Eur J Biochem 209:267–273.

Petrosillo G, Ruggiero FM, Paradies G (2003) Role of reactive oxygen species and cardiolipin in the release of cytochrome c from mitochondria. FASEB J 17:2202–2208.

Said Ahmed M, Hung WY, Zu JS, Hockberger P, Siddique T (2000) Increased reactive oxygen species in familial amyotrophic lateral sclerosis with mutations in SOD1. J Neurol Sci 176:88–94.

Shidoji Y, Hayashi K, Komura S, Ohishi N, Yagi K (1999) Loss of molecular interaction between cytochrome c and cardiolipin due to lipid peroxidation. Biochem Biophys Res Commun 264:343–347.

Subramaniam JR, Lyons WE, Liu J, Bartnikas TB, Rothstein J, Price DL, Cleveland DW, Gitlin JD, Wong PC (2002) Mutant SOD1 causes motor neuron disease independent of copper chaperone-mediated copper loading. Nat Neurosci 5:301–307.

Takeuchi H, Kobayashi Y, Ishigaki S, Doyu M, Sobue G (2002) Mitochondrial localization of mutant superoxide dismutase 1 triggers caspase-dependent cell death in a cellular model of familial amyotrophic lateral sclerosis. J Biol Chem 277:50966–50972.

Trounce IA, Kim YL, Jun AS, Wallace DC (1996) Assessment of mitochondrial oxidative phosphorylation in patient muscle biopsies, lymphoblasts, and transmitochondrial cell lines. Methods Enzymol 264:484–509.

Warita H, Hayashi T, Murakami T, Manabe Y, Abe K (2001) Oxidative damage to mitochondrial DNA in spinal motoneurons of transgenic ALS mice. Brain Res Mol Brain Res 89:147–152.

Wong PC, Pardo CA, Borchelt DR, Lee MK, Copeland NG, Jenkins NA, Sisodia SS, Cleveland DW, Price DL (1995) An adverse property of a familial ALS-linked SOD1 mutation causes motor neuron disease characterized by vacuolar degeneration of mitochondria. Neuron 14:1105–1116.

Xiong Y, Gu Q, Peterson PL, Muizelaar JP, Lee CP (1997) Mitochondrial dysfunction and calcium perturbation induced by traumatic brain injury. J Neurotrauma 14:23–34.

Xu GP, Dave KR, Moraes CT, Busto R, Sick TJ, Bradley WG, Perez-Pinzon MA (2001) Dysfunctional mitochondrial respiration in the wobbler mouse brain. Neurosci Lett 300:141–144.

Yuan H, Williams SD, Adachi S, Oltersdorf T, Gottlieb RA (2003) Cytochrome c dissociation and release from mitochondria by truncated Bid and ceramide. Mitochondrion 2:237–244.